We are IntechOpen,
the world's leading publisher of
Open Access books
Built by scientists, for scientists

6,900
Open access books available

186,000
International authors and editors

200M
Downloads

154
Countries delivered to

Our authors are among the

TOP 1%
most cited scientists

12.2%
Contributors from top 500 universities

BOOK CITATION INDEX
CLARIVATE ANALYTICS
INDEXED

WEB OF SCIENCE™

Selection of our books indexed in the Book Citation Index
in Web of Science™ Core Collection (BKCI)

Interested in publishing with us?
Contact book.department@intechopen.com

Numbers displayed above are based on latest data collected.
For more information visit www.intechopen.com

Electromagnetic Computation of the Short-range Wireless Linkbuget for Biomedical Communication

Ilkyu Kim

Additional information is available at the end of the chapter

Abstract

The biomedical monitoring and imaging system requires data and power transmission through short-range communication, and the interference between large antennas placed within near-field region becomes the important consideration in designing an entire system. For the short-range communication, the electromagnetic computation becomes more complex, which requires huge computational resources. The efficient numerical methods that can be used in short-range communication are (1) Friis formula with correction term and (2) integral coupling formula. Both formulas are similar in an aspect that far-field gain pattern is used to calculate the link budget in a short range. The range of the communication link between two antennas can be defined as reactive near-field, radiating near-field including Fresnel region, a far-field region in the order of nearest distance. Friis formula with correction term can be useful for the simple on-axis antenna displacement in Fresnel region. The integral coupling formula is flexible to compute the mutual coupling of diverse antenna geometries within an entire radiating near-field and a far-field region. Those two methods are evaluated using several examples of short-range communication and interference, and indoor measurement evaluates the validity of the calculated results.

Keywords: mutual coupling, near-field region, Fresnel-field region, far-field region, Friis formula, integral form of coupling formula, biomedical devices, electromagnetic interference (EMI)

1. Introduction

The appearance of body-centric sensing system can realize real-time health care for patients who suffer from several internal diseases. There has been a recent advancement in the biomedical devices for body-centric sensing system. Several researches have been focused

on a new frontier area, such as implanted antenna and wearable antenna for body-centric communication [1–3]. As well as an advancement of biomedical devices, it is also important to maintain a stable communication link between biomedical devices for body-centric sensing system. An accurate operational range of the biomedical devices for power and data telemetry should be determined in an early design process. Recently, low-powered sensor using radio frequency identification (RFID) back-scattering technology has attracted attention due to the concern about the safety issue of patients. The several studies on wireless communication link have been reported in order to realize bio-telemetry. The range of power transmission under the conditions such as in-body, on-body, and off-body has been studied through electromagnetic numerical methods [4]. In addition, it is crucial to predicting the radiative electromagnetic interference (EMI) and adherent strict requirements to avoid the possible interference with other communication links [5–8]. However, most of the evaluation on power transmission has been focused on simple scenarios such as boresight power transmission, and huge computing resources and storage has been involved. An accurate estimation including near-field region was difficult because the interpretation of power transmission in the near-field region is more complicated than one in the far-field region. Therefore, at this moment, the accurate and efficient computation method to estimate the power transmission is more desirable.

2. Wireless communication link

The range of the communication link between two antennas can be defined as reactive near-field, radiating near-field, and a far-field region in the order of nearest distance as shown in **Figure 1**. In the far-field region, it is well-known that the radiation pattern of the antenna is identical regardless of the distance from the antenna. However, in the near-field region, the radiation pattern changes as the distance from the phase center of the antenna changes. Within the near-field region, radiation pattern becomes broadened, and the gain of the antenna is reduced.

It is worth noting that the on-axis power density of the antenna within the Fresnel region decreases monotonically. The approximated on-axis power densities of a radiating aperture varies as [15].

$$|E|^2(R) \propto \left[1 - cos\left(\frac{2D^2/\lambda}{8R}\pi\right)\right]/2 \qquad (1)$$

Figure 1 shows the on-axis power densities of the circular aperture with 10λ diameter. The on-axis power transmission using far-field approximation deviates from both Fresnel and near-field curves. The Fresnel approximation also deviates from near-field curve while it shows its effectiveness beyond the last peak of on-axis power transmission. The Fresnel field region can be approximately defined as the area from the point of the last peak to the far-field edge defined by $2D^2/\lambda$.
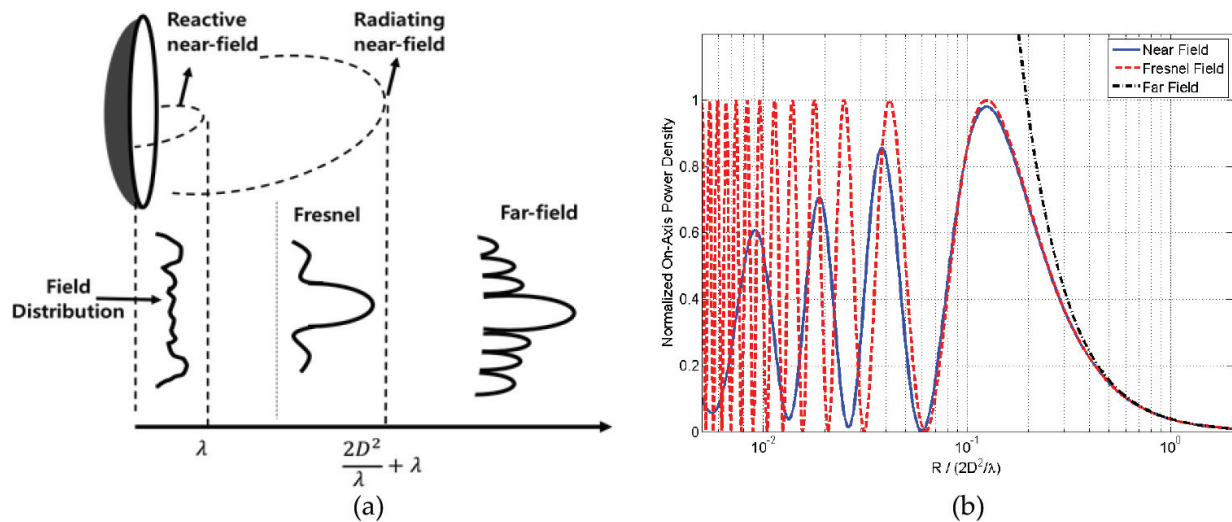
Figure 1. (a) Field distribution for different field ranges and (b) normalized on-axis power density of a uniform circular aperture with 10λ diameter.

Therefore, the distance R of the last peak value can be calculated by.

$$R = \frac{1}{8}\frac{2D^2}{\lambda} = \frac{A}{\lambda\pi} \tag{2}$$

where A is the physical area of the aperture. The definition of Fresnel region would be more accurate including the effects of tapering efficiency and phase errors. Using the definition of the antenna effective area, (2) can be redefined as.

$$R = \frac{A^e}{\lambda\pi} = \frac{\lambda G}{4\pi^2} \tag{3}$$

where the effective area A^e can be defined as $\lambda^2 G/(4\pi)$.

The definition in (3) can be another approach to determine the Fresnel region. The on-axis power densities for several analytical aperture fields were reported in [15], which all confirm the effectiveness of (3).

3. Methods of evaluation on power transmission

The accuracy of the formula can be determined by how well the gain reduction is estimated, compared to the Friis formula. The nearest distance for estimation, flexibility in antenna geometry and computational resources needs to be considered. **Figure 2** presents the flowchart for evaluating the power transmission in near-field and a far-field region. Estimating a power transmission is presented in this chapter using following methods:
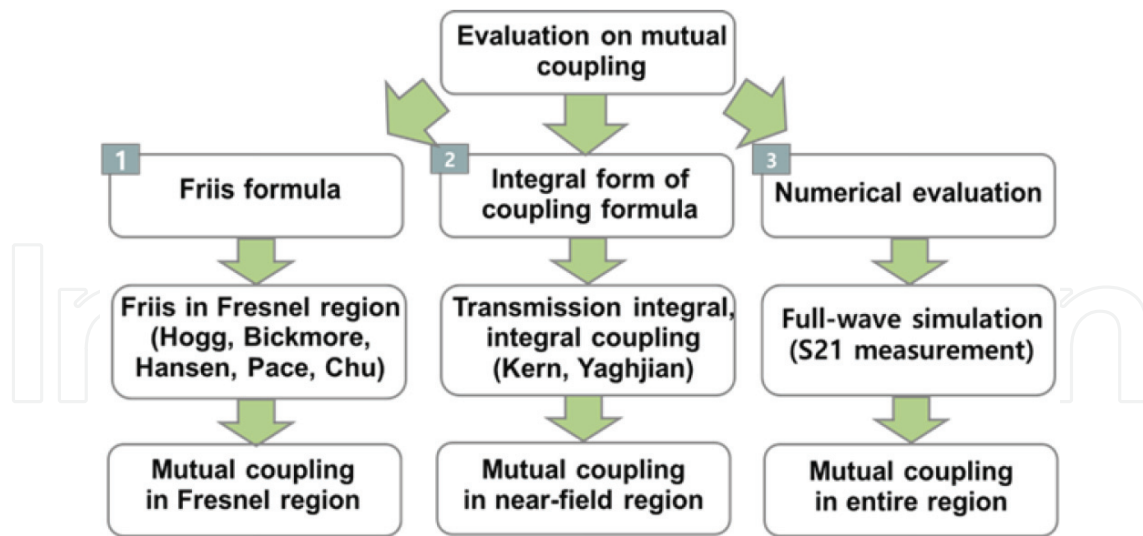
Figure 2. Flowchart of the mutual coupling evaluation in radiating near-field and a far-field region.

1. Friis formula with a correction term

2. The integral form of coupling formula

3. Evaluation using full-wave simulations and indoor measurement.

Those methods are different with respect to (a) possible antenna geometries, (b) required information, and (c) computational resources. The Friis formula can be expressed with a correction term of [11–18]. The formula can accommodate the instant computation with the basic information, such as gain at bore-sight and operational frequency while its effectiveness is confined within the Fresnel region. The integral form of coupling formula [20–24] is expressed with the integral of the scalar products between two far-field patterns. This formula can accommodate an accurate computation within an entire radiating near-field region with reasonable complication. The various antenna scenarios such as rotation and off-axis can be calculated using the formula. Final research method is the use of full-wave simulation and measurement. Recent advancement in computing resources makes it possible to use numerical evaluation such as full-wave simulation. The range of numerical evaluation includes radiative and reactive near-field region while its computation is most complex among three research methods.

4. Friis formula with correction term

4.1. Introduction

The standard Friis formula [9] has been successful in calculating the link budget in wireless communications between two distant antennas. The Friis formula is simple to use and practical to quickly determine the power transmission. Four different methods were used in order to derive the Friis formula, and all results in same conclusion [10]. It is assumed in the derivations that accuracy of the formula is limited to the far-field region. The attempt to predict power

transmission in a Fresnel region has been made through using the concept of gain reduction factor. The gain reduction factor can be defined as the ratio of gain in a near-field region to the gain in the far-field region. Several efforts have been made to present an appropriate model to estimate an accurate gain reduction factor. The defocusing effect in a Fresnel region was derived in the gain reduction factor of uniform and tapered apertures [11]. An asymptotic series with Friis formula and correction term computed on-axis power transmission in a Fresnel region [12]. Gaussian approximation composed of effective aperture area shows its effectiveness for practical use in a Fresnel region [13]. The on-axis Fresnel gain is evaluated [14, 15]. The higher order interaction between two closely spaced horn antennas was investigated, and the power transmission was evaluated [16]. However, there has been limitation with respect to the applications of those proposed formulas, due to the lacking of numerical capabilities at that time. Most of scenarios were focused on simple boresight power transmission. Recent research activities related to the Friis formula were very handful, and its effectiveness was only valid in the far-field region [17, 18].

In this chapter, the power transmission is evaluated using an asymptotic form of the Friis formula [19], which is advantageous with respect to computational complexity, compared to the previous work. The formula is effective in both near-field (Fresnel) and far-field regions. The computation of gain reduction factor depends on the way how to normalize the distance between two antennas. Most of the previous researches have focused on normalization of separation distance in terms of antenna directivity and wavelength. However, using this normalization, gain reduction factor depends on shape and size of antenna aperture. However, by taking a normalization with respect to antenna gain (or effective area) and wavelength, a single gain reduction factor is achieved for any type of antennas. This method may be more useful in the case where the quick and simple calculation is required.

4.2. Standard Friis formula in the far-field region

Figure 3 depicts the antenna geometry where a receiving antenna is placed in the far-field or in the Fresnel region of transmitting antennas. The ratio of receiving power to the transmitting power (P_r/P_t) between two antennas in the far-field region can be obtained using the Friis formula.

$$\frac{P_r}{P_t} = \frac{\lambda^2}{16\pi^2 R^2} G_t(\theta_t, \phi_t) G_r(\theta_r, \phi_r) \left(1 - |\Gamma_t|^2\right) \left(1 - |\Gamma_r|^2\right) |\widehat{\rho}_t \cdot \widehat{\rho}_r|^2 \tag{4}$$

where $G_t(\theta, \phi)$: the far-field gain pattern of transmitting antenna,

$G_r(\theta, \phi)$: the far-field gain pattern of receiving antenna,

$1 - |\Gamma|^2$: input impedance mismatch,

$|\widehat{\rho}_t \cdot \widehat{\rho}_r|^2$: the polarization mismatch.

R is the separation distance measured between the phase centers of the Tx and Rx antennas, and the far-field gain pattern differs depending on the angular direction. The relationship between the mutual coupling $|S_{21}|$ and the ratio of P_r/P_t can be defined as.

$$|S_{21}| = \sqrt{\frac{P_r}{P_t}} \qquad (5)$$

The radiation patterns of two antennas are important to determine the power transmission between two antennas. A receiving antenna is placed at the distance of near-field or far-field of the other antenna. The on-axis power transmission between two antennas is evaluated with full-wave simulation and Friis formula. The standard Friis formula shows its effectiveness in the far-field region while degradation of the accuracy is observed in the near-field region. The difference between two results grows as one antenna is located closer to the other antenna. **Figure 3** shows a comparison of power transmission of horn antennas and simulated result exhibits a huge deviation from the Friis formula which is equivalent to 5 dB at $R = 2\lambda$. The main reason resulting in the deviation is that the Friis formula only uses the far-field gain. However, the actual gain pattern in the Fresnel region depends on different distances from the antenna phase center.

4.3. Friis formula in the Fresnel region

As previously mentioned, the accuracy of the standard Friis formula deteriorates at close distances. Its accuracy can be improved by incorporating the distance-dependent antenna gain variations in the Fresnel region. By replacing the far-field antenna gains used in (4) with the gain variations in the Fresnel region $G_F(R)$, a Friis formula in the Fresnel region is obtained as,

$$\frac{P_r}{P_t} = \frac{\lambda^2}{16\pi^2 R^2} G_{F,t}(R) \, G_{F,r}(R) \qquad (6)$$

It is worth noting that the gain variations in Fresnel region are now a function of R. A gain reduction factor γ usually represents the gain decrease effect in the Fresnel region, which is the ratio between the antenna gains in the Fresnel and one in the far-field regions. It can be defined as.

$$\gamma(R) = \frac{G_F(R)}{G} \qquad (7)$$

Using (7), the formula can be rewritten as.

$$\frac{P_r}{P_t} = \frac{\lambda^2}{16\pi^2 R^2} \gamma_t(R) \, G_t \, \gamma_r(R) \, G_r \qquad (8)$$

Eqs. (7) and (8) assumes that it is possible to separate the gain reduction factor for each individual antenna, and they can be obtained through analytical derivation, full-wave simulations or measurements of the antenna gain pattern. [12] suggested that an antenna gain in the Fresnel region can be approximated with a quadratic form of variation in terms of its far-field gain:

$$\gamma(\Delta) = \frac{G_F(\Delta)}{G} = 1 - \alpha\Delta^{-2} + O(\Delta^{-4}) \qquad (9)$$

where Δ: the normalized form of the distance R between two antennas, α: a coefficient that determines the reduction rate of the antenna gain.
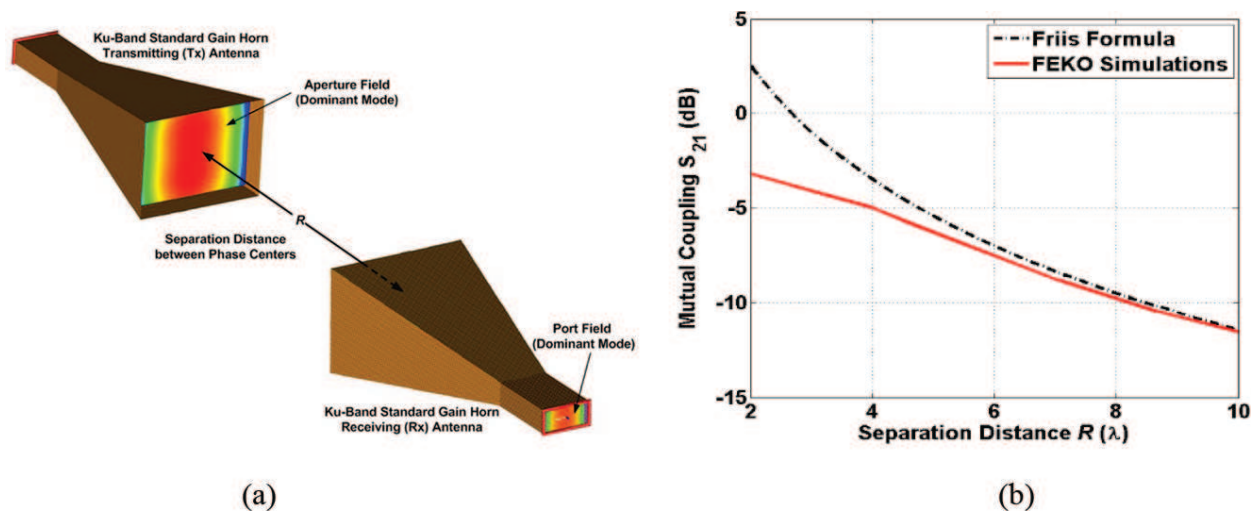
Figure 3. (a) On-axis mutual coupling between two Ku-band horn antennas and (b) failure of standard Friis formula in near-field region.

In general, the gain reduction factor α may be different for different types of antennas with a conventional definition of normalized distance R. The conventional derivation utilized far-field edge distance, $(2D^2/\lambda)$ to normalize separation R. However, with a new derivation of the normalized separation R. distance Δ, a single coefficient α for various types of antennas can be obtained. The assumption used in the derivation is that physical area of the aperture A in (11) can be replaced by its effective area A_e. This method would be more realistic so that the effects of operating frequency, antenna size, and tapering efficiency can all be included in Δ. This may be able to result in a more single α. It is supposed that input impedances are matched and the two antennas are aligned in boresight direction with matched polarization.

$$\Delta = \frac{R}{2\lambda G/\pi^2} \ \text{(Proposed normalization)} \tag{10}$$

$$\Delta' = \frac{R}{2D^2/\lambda} \ \text{(Conventional normalization)} \tag{11}$$

where G: the antenna gain in the far-field region, R: the separation distance between two antennas.

The proposed method utilizes the separation distance Δ, normalized with respect to the antenna gain (or the effective area) and wavelength. Using the definition of normalization, we follow the quadratic asymptotic form of the gain reduction factor used in literature an propose a novel normalization form of separation distance R.

4.4. Gain reduction factor in the Fresnel region

Using proposed normalization in (10), more converged curves are observed for aperture antennas such as horns and reflectors. The effectiveness of $2\lambda G/\pi^2$ proposed normalization is validated through these examples. However, except for the aperture antennas, it does not provide enough convergence for relatively low-gain antennas such as small dipoles and open-ended waveguides. This is because the far-field gain G used in (10) is defined as one of
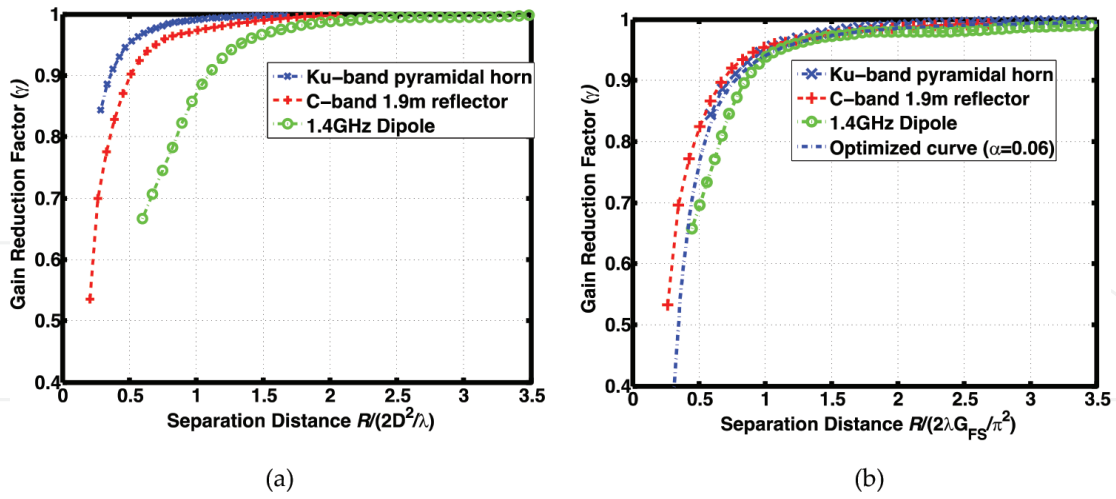
Figure 4. The gain reduction factor (a) using normalized distance R with respect to $2D^2/\lambda$ and (b) using normalized distance R with respect to $2\lambda G_{FS}/\pi^2$ (right).

the aperture antenna, which is well-known to radiate toward the direction of front-side of the aperture. Thus, in order to include the low-gain antennas, the modified antenna gain can be defined using total radiated power over a half sphere. The modified gain, namely the front-side gains G_{FS}, can be used instead of the far-field gain G presented in (10). The front-side gain and associated gain reduction factor can be expressed as:

$$G_{FS} = \frac{4\pi U_m}{P_F}, \qquad \gamma_{FS}(\Delta) = 1 - \alpha_U \left(\frac{R}{2\lambda G_{FS}/\pi^2}\right)^{-2} \qquad (12)$$

where U_m: the maximum radiation intensity, P_F: the total radiated power over a half sphere where maximum occurs.

Figure 4 shows the gain reduction factors using the front-side gain, which can achieve sufficient convergence of all curves. The trend of all the curves suggests that an empirical coefficient α can be $\alpha = 0.06$. The major weakness of this method is that we need to calculate the front-side gain, based on complex 3D radiation pattern.

Instead of using front-side gain, the simpler adjusted gain would be more desirable with respect to the instant calculation of the mutual coupling. The proposed antenna gain can be obtained depending on its classification: low-gain or high-gain antennas defined as below:

$$G_A = G \ (G \geq 10 \ \text{dB} : \text{high } G) = G + 3 \ \text{dB} \ (G < 10 \ \text{dB} : \text{low } G), \gamma_A(\Delta) = 1 - \alpha_U \left(\frac{R}{2\lambda G_A/\pi^2}\right)^{-2} \quad (13)$$

where G_A is the proposed adjusted gain.

Otherwise, more sophisticated switching model can be used such as:

$$\gamma_A(\Delta) = 1 - \alpha_U F(G) \left(\frac{R}{2\lambda G_A/\pi^2}\right)^{-2}, \quad F(G) = 2.5 - \frac{a}{\pi} \cdot arctan[c \cdot (G - b)] \qquad (14)$$

where the constant is found to be $a = 3$, $b = 10$, and $c = 1$.

Note that the adjusted gain G_A is recommended after an empirical case studies. It is also verified that the proposed method in (13) also exhibits similar convergence to the result of (12). It implies that the empirical coefficient α for (13) can be obtained as $\alpha = 0.06$ for the class of the various antennas. The numerous case studies suggest that maximum deviation of gain reduction factor can be converted into 0.5 dB error in power level. The effectiveness of the gain reduction factor will be discussed evaluating the power transmission in following sections.

5. Integral form of coupling formula

5.1. Introduction

Another method to evaluate mutual coupling is the use of integral form of coupling formula, which is advantageous in its flexibility. The power transmission for various antenna geometries such as rotation and offset in a closer distance maybe required for a comprehensive coupling evaluation. The formula is advantageous since it estimates the coupling in the very close distance, which covers an entire radiating near-field region. The integral form of coupling formula takes a form of a scalar integral of two vector far-field patterns. Transmission integral was studied, which is based on plane-wave scattering matrix (PWSM) theory, and its validity is evaluated through the power transmission between two identical apertures [20]. Two different computer programs were developed to calculate the coupling between two antennas located in a longitudinal and transverse displacement [21]. The coupling in both near-field and far-field is evaluated. The measured far-fields of array and reflector antennas are used for the calculation of near-field pattern [22]. An advancement in computer program increases freedom of possible antenna orientation and displacement [23, 24].

5.2. Integral form of coupling formula

The integral form of coupling formula is practical and flexible, which enables to calculate power transmission in diverse scenarios such as rotation and off-axis cases. The complexity of required information slightly increases, compared to the Friis formula with a correction term. While simple bore-sight gain and antenna geometry are employed in Friis formula, the integral form of coupling formula utilizes 3D vector far-field patterns of two antennas and antenna displacement. Several cases are studied using the integral form of coupling formula and validity of the result is evaluated comparing with the full-wave simulation FEldberechnung für Körper mit beliebiger Oberfläche (FEKO).

The ratio between input wave and output wave presented in [21, 22] can be expressed as normalized vector far-field pattern of transmit antenna $\bar{f}_{TX}(\bar{k})$ and receive antenna $\bar{f}_{RX}(-\bar{k})$.

$$\frac{b'_0}{a_0}(R) = -\frac{C}{4\pi k} \iint_{\sqrt{k_x{}^2 + k_y{}^2} < k} \frac{\bar{f}_{Tx}(\bar{k}) \cdot \bar{f}_{RX}(-\bar{k})}{k_z} e^{-j\bar{k}\cdot\bar{r}} \, dk_x dk_y \tag{15}$$

a_0 is the amplitude of input wave of transmitting antenna, b_0 is the amplitude of output wave of receiving antenna, and $\bar{k}$ is the wave vector. The Eq. (15) has e^{jwt} time dependence in free space, and the constant C can defined as:

$$C = -\frac{Z_{wg,Rx}}{Z_0} \frac{1}{1 - \Gamma_{L,Rx}\Gamma_{0,Rx}} \tag{16}$$

$Z_{wg,Rx}$, Z_0 are the impedance of feed waveguide in receive antenna and free space impedance. $\Gamma_{L,Rx}$, $\Gamma_{0,Rx}$ are reflection coefficient of the load impedance and the receive antenna impedance, respectively. The discretization of the sampling space k_x-k_y and discrete Fourier transform is required in order to obtain the coupling quotient, and the sampling frequency is defined as

$$f_s = 2\kappa \times (D_{Tx} + D_{Rx}) \tag{17}$$

D_{Tx} and D_{Rx} are the diameters of a sphere, which encloses the geometry of transmit and receive antenna, respectively. The constant κ is the oversampling ratio, which limits the movement of antennas in the transverse direction. The separation distance between two antennas can also be defined as:

$$\frac{D_{Tx} + D_{Rx}}{2} \leq R \leq \frac{(D_{Tx} + D_{Rx})^2}{2} \tag{18}$$

At the minimum separation distance, the accuracy deteriorates due to the growing reactive field component. When R approaches the maximum separation distance, the only near-axis plane wave is taken into consideration, which leads to the inaccurate result of calculation [22].

6. Evaluation using numerical methods

6.1. Evaluation using Friis formula with a correction term

The on-axis power transmission between two identical antennas is evaluated at various separation distances. Both far-field antenna gain of the antenna and separation distance is required information. In addition, the point of phase center is important to measure the accurate separation distance. The first example is selected as two half-wavelength dipole antennas, which operate at 1.4GHz with the far-field gain of 2.14 dB. The next example uses two standard gain horns at 12.7GHz with the far-field gain of 15.2 dB, and the phase center of the horn antenna is located at 5 mm below the antenna aperture.

$$\frac{P_r}{P_t} = \frac{\lambda^2 G_t G_r}{16\pi^2 R^2} \left(1 - \alpha_E \left(\frac{R}{2\lambda G/\pi^2}\right)^{-2}\right) \left(1 - \alpha_E \left(\frac{R}{2\lambda G/\pi^2}\right)^{-2}\right)$$
$$\times \left(1 - |\Gamma_t|^2\right) \left(1 - |\Gamma_r|^2\right) |\widehat{\rho}_t \cdot \widehat{\rho}_r| \tag{19}$$

The coupling level is obtained using the Friis formula with correction term, and the validity of the formula is evaluated by comparing it with the full-wave simulation FEKO. The comparison among standard Friis formula, Friis formula with correction term (asymptotic Friis formula),
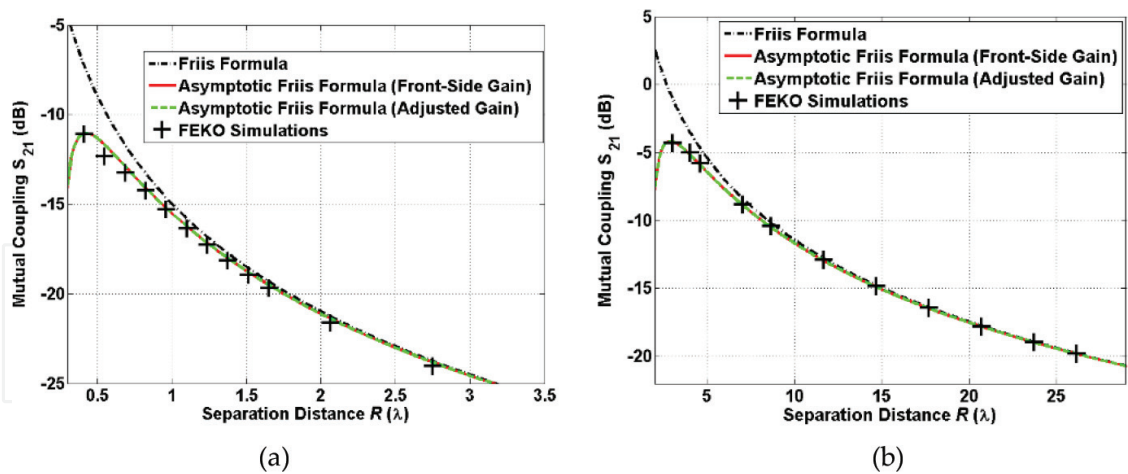
Figure 5. (a) Mutual coupling between two dipole antennas operated at 1.4GHz and (b) mutual coupling between two Ku-band horn antennas operated at 12.7GHz.

and simulated results is made as shown in **Figure 5**. The Friis formula with correction term agrees well with the simulated coupling level. In addition, it does provide a significant enhancement after the nearest distance of Fresnel region while the standard Friis formula results in huge deviation. However, it is also shown that the calculated result drops drastically before the nearest distance of Fresnel region, which indicates that its effectiveness is limited to the Fresnel region and far-field region. The formula is made up of quadratic form of the gain reduction factor, which turns out to be negative at a very close distance. In order to predict the coupling at a closer distance, higher order term of interaction should be considered in the quadratic form of gain reduction factor. The nearest prediction ranges for the high-gain antenna is around $1.44 \times (D^2/2\lambda)$. The nearest range for dipole antenna is approximately 0.35λ.

6.2. Evaluation using integral form of coupling formula

The first step is to obtain the 3D vector far-field pattern with phase and amplitude using FEKO. Next step is to take the integral of scalar product between two far-field patterns so that the coupling with respect to the antenna geometries can be calculated. For the purpose of evaluation, 2 m and 1.9 m prime-focus reflector operated at 5.5GHz are used as an example. The far-field pattern is simulated using FEKO, and the maximum directivity of 42.5 dB and 42.1 dB is obtained for each reflector antenna, respectively. Integral coupling formula is calculated for the bore-sight scenario using the far-field patterns of both antennas. The calculated result is compared to the Friis formula and FEKO simulation as shown in **Figure 7**. The integral coupling agrees well with the FEKO simulation within 0.5 dB deviation. It is worthy noting that the formula is effective within the radiating near-field region, and no sudden decrease of the coupling level in the nearest distance is observed. The second example is selected as the ground station antennas pointing to the multiple satellites. The interference between two antennas is investigated using the integral form of a formula. In order to communicate with satellites, antennas are both tilted at $\theta = 45°$ toward the sky, and the separation

of two antennas is around 3 m. The configuration of both antennas is also shown in **Figure 6**. In a similar way, coupling integral is calculated, and the comparison of the results is shown in **Table 1**. Considering that the cross-pol component becomes significant in off-axis radiation pattern, the comparison shows reasonable agreement within 3 dB difference.

(a)   (b)
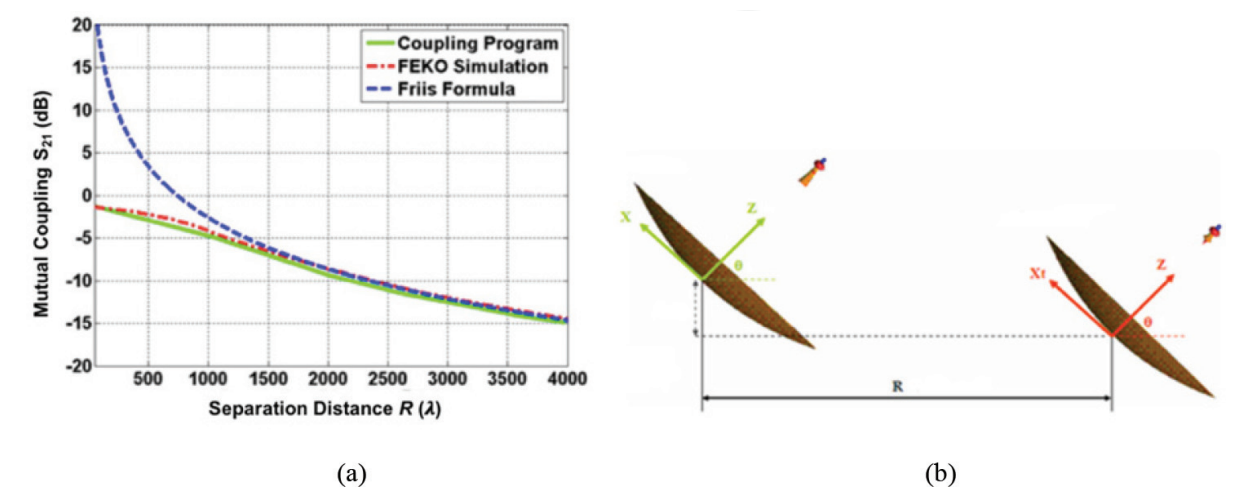
Figure 6. (a) On-axis mutual coupling between C-band 2 m and 1.9 m reflector antennas and (b) off-axis mutual coupling between the two reflector antennas.

(a)   (b)
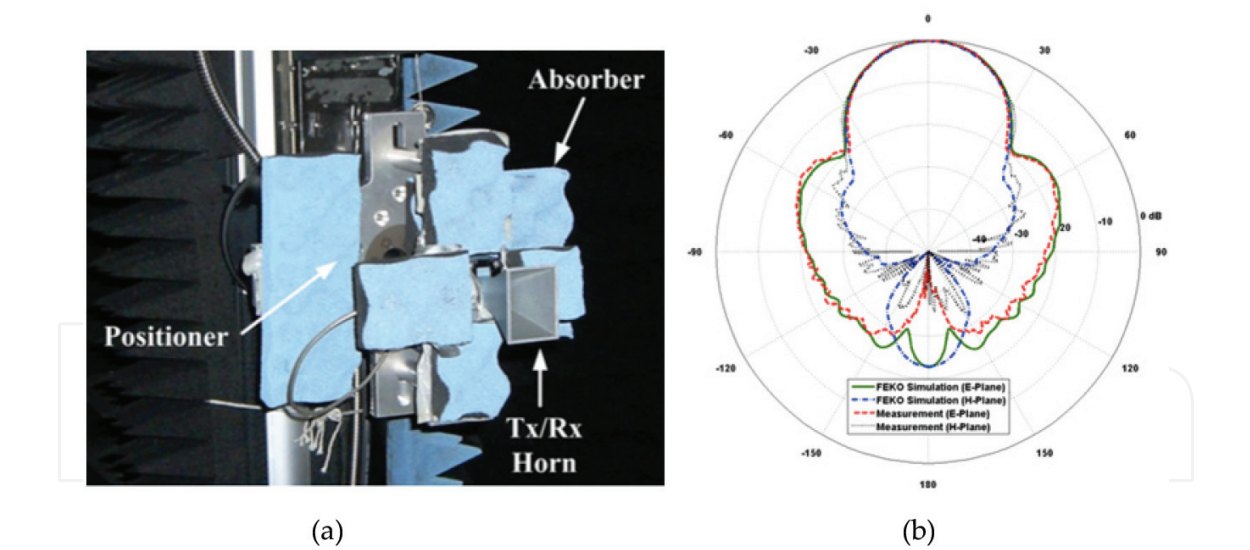
Figure 7. (a) Setup of horn antenna inside near-field anechoic chamber and (b) far-field radiation pattern from the measurement.

	FEKO	**Integral coupling**
Coupling level	−77.14 dB	−80.81 dB

Table 1. Off-axis mutual coupling between the two reflector antennas.

## 7. Evaluation using the two numerical methods

7.1. Evaluation using mutual coupling measurement

The coupling level between two identical Ku-band standard gain horns is measured in order to evaluate the proposed formula. The standard gain horn operates at 12.7GHz, the center frequency of Ku-band, and the radius of the sphere, which encloses the horn antenna, is around 2.15λ. The radiation pattern of the Ku-band standard gain horn is measured inside the UCLA spherical near-field range as shown in **Figure 7**. The amplitude and phase of the radiated near-field are acquired by rotating the horn mounted on the positioner. The near-field information can be converted into far-field radiation pattern. The comparison between measured far-field and the simulated far-field pattern using FEKO is depicted in **Figure 8**. The max simulated and measured gain patterns are 15.28 dB and 15.47 dB, respectively.

As shown in **Figure 8**, the two horn antennas are mounted on an optical table and the mutual coupling S_{21} is measured using a vector network analyzer. To properly measure S_{21}, we need to carefully setup the measurement as below:

1. The polarization of both horn antennas must be perfectly matched in order to avoid any loss due to the mismatch of polarization.

2. The insertion loss proportional to the length of cable should be carefully measured and counted in calculating the coupling level.

3. Separation distance R needs to be measured from one phase center to the other phase center. Prior to measuring the distance, it is critical to determine the phase center where the phase response of far-field pattern is uniform. In general, the simulated model can be used to find the location of the phase center.

The separation distance R varies from 4 to 31λ in the on-axis direction. The mutual coupling levels using different methods are compared as shown in **Figure 8**. The simulated results show

(a)   (b)
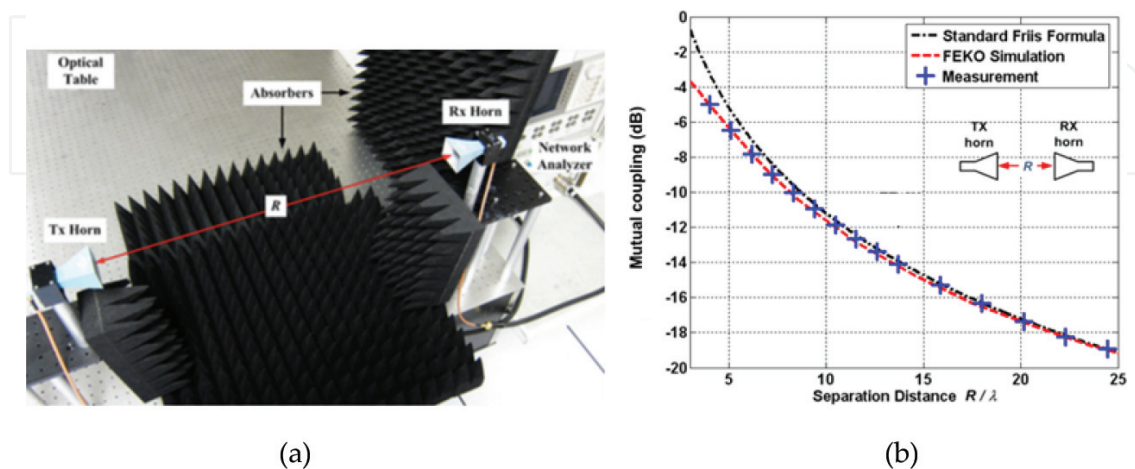
Figure 8. (a) Indoor measurement of mutual coupling and (b) measured mutual coupling level in order to evaluate the simulated coupling level.
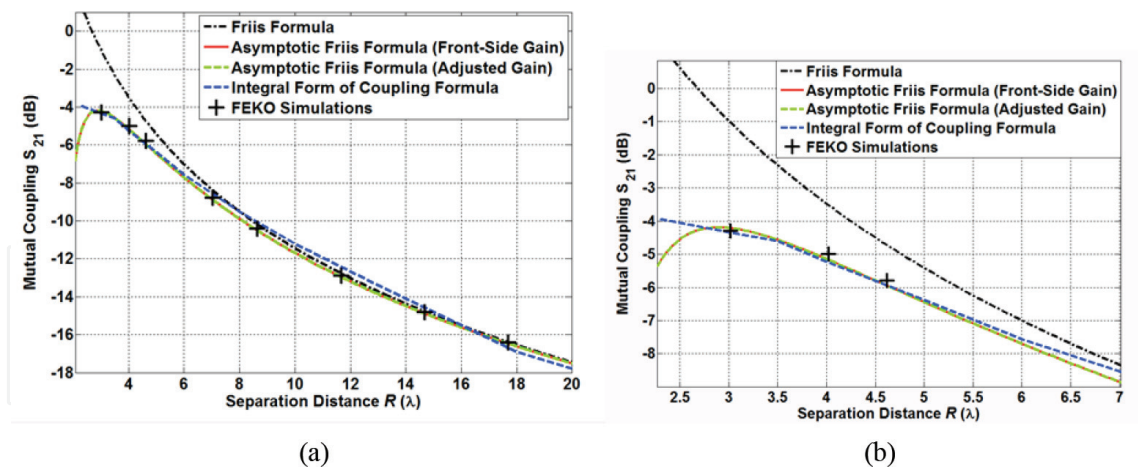
Figure 9. (a) Evaluation using Friis formula, asymptotic Friis formula, integral form of coupling formula, and FEKO simulation and (b) close up in the radiating near-field region.

a good agreement with the measurements. It can be concluded that the validity of the simulation is successfully evaluated with the measurement.

7.2. Error analysis of the two numerical methods

An error of the proposed numerical methods is evaluated with respect to the full-wave simulation. The mutual coupling between identical Ku-band horn antennas is computed using the two methods: (1) Friis formula with gain reduction factor and (2) Integral form of coupling formula. The graphs of the proposed methods and measurement are shown in **Figure 9**. It is worthy noting that the proposed two methods are all effective within Fresnel region while the integral coupling formula extends its effectiveness to the radiating near-field region. The mutual coupling of the asymptotic Friis formula and integral form of coupling formula deviates from the simulated one at the distance of less than $R = 3\lambda$ and $R = 2.3\lambda$, respectively. Beyond the each nearest separation distance, it is observed that maximum error with respect to the simulated result is less than 0.5 dB, which corresponds to around 11% deviation in power level. It verifies that the two numerical methods can provide the reasonable agreement with respect to the full-wave simulation.

8. Conclusion

The mutual coupling between one antennas placed in radiating near-field and far-field ranges of the other antenna is calculated using proposed formulas and evaluated through full-wave simulation and measurement. It is shown that those formulas enable to provide enhancement in the radiating near-field region in comparison to the standard Friis formula. The optimal formula can be selected depending on the availability of input information, the proximity of range, and the flexibility of antenna geometry. The important features of those two formulas are summarized in **Table 2**. The validity of simulated mutual coupling level is evaluated through the measurement. The setup of indoor measurement is discussed, and the key factors to affect the accuracy of the

measurement are addressed. Those methods can be also expanded to the antenna measurement and near-field applications.

	Friis formula with correction term	Integral form of coupling formula	Full-wave simulation
Required information	Low	High	—
Proximity of range	Fresnel region	Radiating near-field	Entire near-field
Flexibility of geometry	Low	High	High

Table 2. Comparison of the proposed numerical methods.

Author details

Ilkyu Kim

Address all correspondence to: ilkyukim@gmail.com

Defense Agency for Technology and Quality, South Korea

References

[1] Izdebski P, Rajagopalan H, Rahmat-Samii Y. Conformal ingestible capsule antenna: A novel chandelier meandered design. IEEE Transactions on Antennas and Propagation. April 2009;**57**(4):900-909

[2] Esko S, Jouni K, Juha P, Arto Y, Ilkka K. Application of near field communication for health monitoring in daily life. IEEE Proceeding 28th Annual International Conference Engineering in Medicine and Biology Society. August 2006:3246-3249

[3] Rao S, Llombart N, Moradi E, Koski K, Bjorninen T, Sydanheimo L, Rabaey J, Carmena J, Rahmat-Samii Y, Ukkonen L. Miniature implantable and wearable on-body antennas: Toward the new era of wireless body-centric. IEEE Antennas and Propagation Magazine. February 2014;**56**(1):271-291

[4] Wilson PF, Hill DA, Holloway CL. On determining the maximum emissions from electrically large sources. IEEE Transactions on Antennas and Propagation, August. 2002;**44**(1):79-86

[5] Hernando MM, Fernandez A, Arias M, Rodriguez M, Alvarez Y, Las-Heras F. EMI radiated noise measurement system using the source reconstruction technique. IEEE Transactions on Industrial Electronics. August, 2008;**55**(9):3258-3265

[6] Tarusawa Y, Ohshita K, Suzuki Y, Nojima T, Toyoshima T. Experimental estimation of EMI from cellular base-station antennas on implantable cardiac pacemakers. IEEE Transactions on Electromagnetic Compatibility. November, 2005;**47**(4):938-950

[7]   Lee SG, Hoang H, Choi YH, Bien F. Efficiency Improvement for Magnetic Resonance Based Wireless Power Transfer with Axial-misalignment. Electronics Letters. 6, March 2012;**48**:339-340

[8]   Kim J, Rahmat-Samii Y. "Implanted antennas inside a human body: simulations, designs and characterizations," IEEE Transactions on Microwave Theory and Techniques, August 2004;**52**(8):1934-1943

[9]   Friis GHT. A note on a simple transmission formula. Proceedings of the IRE. May 1946;**34**: 254-256

[10] Hogg DC. Fun with the Friis free-space transmission formula. IEEE Antennas and Propagation Magazine. August 1993;**35**(4):33-35

[11] Soejima T. Fresnel gain of aperture aerials. Proceedings of the IEE. June 1963;**110**(6):1021-1027

[12] Pace JR. Asymptotic formulas for coupling between two antennas in the fresnel region. IEEE Transactions on Antennas and Propagation. May 1969;**AP-17**(3):285-291

[13] Chu TS. An Approximate generalization of the Friis transmission formula. Proceedings of the IEEE. March 1965:296-297

[14] Polk C. Optical Fresnel-region gain of a rectangular aperture. IRE Transactions on Antennas and Propagation. January 1956;**AP-4**:65-69

[15] Bickmore RW, Hansen RC. Antenna power densities in the Fresnel region. Proceedings of the IRE (Correspondence). December 1959;**47**:2119-2120

[16] Iskander M, Hamid M. Numerical solution for the near-field transmission between two H-plane sectoral electromagnetic horns. IEEE Transactions on Antennas and Propagation. January 1976;**AP-24**(1):87-89

[17] Pozar DM. Closed-form approximations for link loss in a UWB radio system using small antennas. IEEE Transactions on Antennas and Propagation. January 2003;**51**(9):2346-2354

[18] Promwong S, Hachitani W, Ching GS, Takada J. Characterization of ultra-wideband antenna with human body. IEEE International Symposium on Communications and Information Technology, ISCIT. July 2004;**2004**

[19] Kim I, Xu S, Rahmat-Samii Y. Generalized correction to the Friis formula: Quick determination of the coupling in the Fresnel region. IET Microwave Antennas And Propagation. Oct. 2013, 7, 1101;**13**:1092

[20] Kerns DM. Plane-wave scattering matrix theory for antenna-antenna interactions. National Bureau of Standards Monograph. 1981;**162**:5-51

[21] Stubenrauch C, Francis M. Comparison of measured and calculated mutual coupling in the near field between microwave antennas. IEEE Transactions on Antennas and Propagation. July 1986;**34**(7):952-955

[22] Yaghjian AD. Efficient computation of antenna coupling and fields within the near-field region. IEEE Transactions on Antennas and Propagation. January 1982;**AP-30**(1):113-128

[23] Akgiray A, Rahmat-Samii Y. Mutual coupling between two arbitrarily oriented and positioned antennas in near- and far-field regions. 2010 URSI International Symposium on Electromagnetic Theory (EMTS); August 2010

[24] Kim I, Rahmat-Samii Y. Calculation of Mutual Coupling between Two Antennas for Satellite Communication. 2016 AP-RASC; August 2016